High resolution digital holographic microscopy with a wide field of view based on a synthetic aperture technique and use of linear CCD scanning

Jianglei Di, Jianlin Zhao,* Hongzhen Jiang, Peng Zhang, Qi Fan, and Weiwei Sun

Institute of Optical Information Science and Technology, Shaanxi Key Laboratory of Optical Information Technology, School of Science, Northwestern Polytechnical University, Xi'an 710072, China

*Corresponding author: jlzhao@nwpu.edu.cn

Received 3 April 2008; revised 30 July 2008; accepted 1 September 2008; posted 16 September 2008 (Doc. ID 94242); published 16 October 2008

Theoretical analysis shows that, to improve the resolution and the range of the field of view of the reconstructed image in digital lensless Fourier transform holography, an effective solution is to increase the area and the pixel number of the recorded digital hologram. A new approach based on the synthetic aperture technique and use of linear CCD scanning is presented to obtain digital holographic images with high resolution and a wide field of view. By using a synthetic aperture technique and linear CCD scanning, we obtained digital lensless Fourier transform holograms with a large area of 3.5 cm × 3.5 cm (5000 × 5000 pixels). The numerical reconstruction of a 4 mm object at a distance of 14 cm by use of a Rayleigh–Sommerfeld integral shows that a theoretically minimum resolvable distance of 2.57 μm can be achieved at a wavelength of 632.8 nm. The experimental results are consistent with the theoretical analysis. © 2008 Optical Society of America

OCIS codes: 090.1995, 070.0070, 100.2000, 100.3010, 120.2880.

1. Introduction

Digital holography allows fast, nondestructive, and full-field measurement of samples by which the amplitude and phase information of the recorded optical field can be simultaneously obtained. In recent years digital holography has been widely used in various fields such as shape and deformation measurement [1,2], microscopy [3–9], color display [10,11], information storage [12], object recognition [13,14], information encryption [15,16], and optical scanning holography [17–20]. However, compared with traditional optical holography, the space–bandwidth product (SBP) of a digital holographic system and the resolution of reconstructed images are significantly restricted because of the limited size (generally only several millimeters) and low cutoff frequency (only 100 line pairs/mm) of the CCD cameras, so that it is difficult to obtain a digital holographic image with high resolution and a wide field of view simultaneously. A decrease in the recording distance of holograms helps to increase the numerical aperture of the system and then obtain high resolution, but, at the same time, it also restricts the field of view. Haddad *et al.* [4] recorded a digital lensless Fourier transform hologram and demonstrated a minimum resolvable distance of 1.4 μm with a wavelength of $\lambda = 514.5$ nm. Takaki and Ohzu [5] proposed a numerical reconstruction method for hybrid holographic microscopy and demonstrated the numerical reconstruction of 1 μm size objects with a wavelength of $\lambda = 632.8$ nm. In the above experiments, the CCD cameras were placed close to the objects (less than 1 cm) to obtain high resolution and so the sizes of the recorded objects (only several micrometers) were limited. Although digital holographic microscopy, in which a microscope objective is introduced to magnify the object wave field, is able to achieve a spatial resolution approaching the diffraction limit, the field of view of the reconstructed images is usually small (less than 100 μm). So to

0003-6935/08/305654-06$15.00/0

increase the area and the pixel number of the recorded digital hologram is an effective approach to increasing the resolution and the field of view of the reconstructed image simultaneously, which allows a large numerical aperture at a long recording distance. However, because of the limitation of the current technology, the commercially available two-dimensional CCD is usually not more than 4000×3000 pixels. To enlarge the area of the digital hologram, the synthetic aperture technique has been used to compose a larger hologram from several recorded holograms with different positions of the same CCD area [21], or to synthesize the reconstruction from multiple holograms (of a scanned wavelength) to achieve improved axial resolution [22]. Moreover, for a linear CCD, it is easy to obtain more than 20,000 pixels in one dimension. That means a digital hologram with an area as large as $20,000 \times 20,000$ pixels might be obtained by using linear CCD scanning (push-broom technology) and a synthetic aperture technique. We present the theoretical analysis and experimental results of this new synthetic aperture technique. Large digital lensless Fourier transform holograms with an area of $3.5\,\mathrm{cm} \times 3.5\,\mathrm{cm}$ (5000×5000 pixels) were recorded by use of linear CCD scanning at a distance of 14 cm. After numerical reconstruction using the Rayleigh–Sommerfeld integral, the digital holographic image of a 4 mm object with a theoretically minimum resolvable distance of $2.57\,\mu\mathrm{m}$ is achieved. We show that the resolution and the wide field of view of the digital holographic image can be simultaneously improved by increasing the equivalent CCD area and the SBP of the holographic system.

2. Experimental Setup

Figure 1 shows the experimental setup for recording lensless Fourier transform holograms based on a synthetic aperture technique by use of linear CCD scanning. A thin laser beam ($\lambda = 632.8\,\mathrm{nm}$) is divided into two parts by beam splitter BS_1. Beam 1 is expanded by microscope objective MO_1 as reference beam R. Beam 2 is expanded and collimated by microscope objective MO_2 and lens L, and then illuminates the object as object beam O. Reference beam R and object beam O interfere in the target plane of the linear CCD (5000 pixels, pixel size of $7\,\mu\mathrm{m} \times 7\,\mu\mathrm{m}$) and the lensless Fourier transform holograms are recorded by use of linear CCD scanning. The object and the reference point source have the same distance to the hologram. A precision translation stage with a step size of $0.625\,\mu\mathrm{m}$ used to control the motion of the CCD is positioned vertically on the optical table. The linear CCD is positioned on the stage with its pixel arrays in the horizontal direction. The illustration of the hologram recording process based on linear CCD scanning is shown in Fig. 2. The precision translation stage is automatically controlled by computer to move in the y direction with a constant velocity of $6.863 \times 10^{-4}\,\mathrm{m/s}$, and the linear CCD is triggered to frame a picture every 0.0102 s. In 51 s we recorded 5000 pictures and then orderly patched them to form a 5000×5000 pixel digital hologram with a large area of $3.5\,\mathrm{cm} \times 3.5\,\mathrm{cm}$.

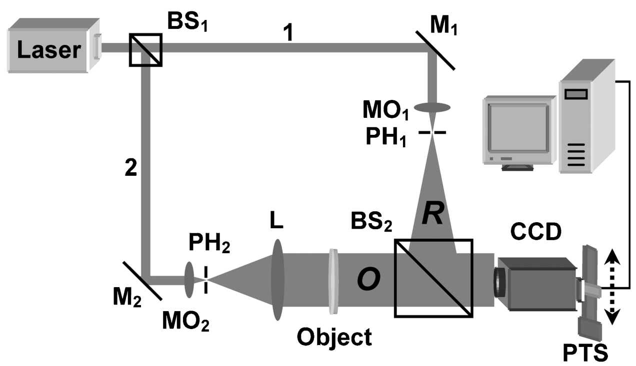

Fig. 1. Experimental setup for recording lensless Fourier transform holograms based on a synthetic aperture technique and use of linear CCD scanning.: BS_1, BS_2, beam splitters; M_1, M_2, mirrors; MO_1, MO_2, microscope objectives; PH_1, PH_2, pinholes; L, lens; CCD, linear CCD camera; PTS, precision translation stage.

In general, the information transfer and processing capability of a digital holographic system can be characterized by its SBP [23]. For a given object, the SBP of a digital holographic system must be larger than a specific value to hold all the information in a digital holographic system, which is always limited by the SBP of the CCD. Lensless Fourier transform holography requires the lowest SBP compared with inline and off-axis holography. As is shown in Fig. 3, the SBP for a given object is denoted as $SW_0 = S_0 W_0$, where S_0 and W_0 are the lateral dimension and the spatial frequency bandwidth of the object, respectively. If M_0 is an arbitrary point in the object plane with the lateral position x_0 and the spatial frequency f_0, the lateral position of point M in the hologram plane located at a distance d from the object under the Fresnel approximation can be given by

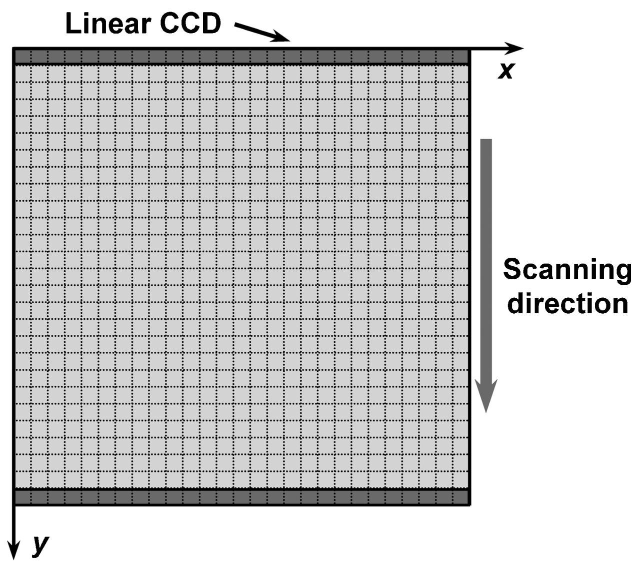

Fig. 2. Illustration of the hologram recording process based on the synthetic aperture technique and use of linear CCD scanning.

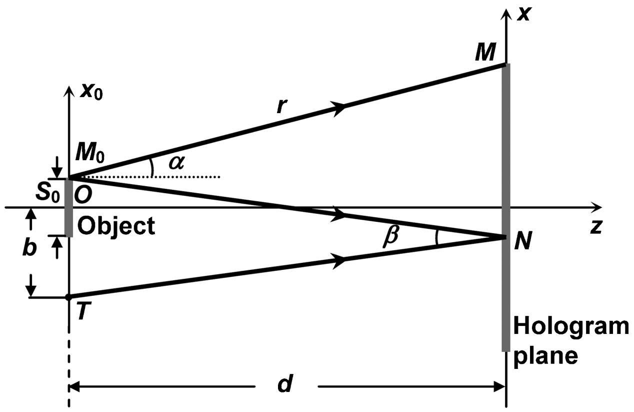

Fig. 3. Principle of lensless Fourier transform holography.

$$x = x_0 + d\alpha = x_0 + \lambda d f_0, \qquad (1)$$

where λ is the wavelength and α is the diffractive angle of the object beam. The lateral dimension of the hologram is accordingly obtained by

$$L = S_0 + \lambda d W_0. \qquad (2)$$

Distance b from reference source T to origin O must satisfy $b \geq 3S_0/2$ to ensure that the zero-order diffraction and the reconstructed images are entirely separated. Hence the maximal angle between the reference wave and the object wave is $\beta = (2b + S_0)/2d$ and the spatial frequency bandwidth of the interference patterns in the hologram plane is

$$W \geq \frac{4S_0}{\lambda d}. \qquad (3)$$

The SBP of the interference wave field in the x direction in the hologram plane can be described by

$$\mathrm{SW} = \mathrm{LW} \geq 4\mathrm{SW}_0 + \frac{4S_0^2}{\lambda d}. \qquad (4)$$

Inequality (4) gives the lowest requirement for the SBP of the recording system for a lensless Fourier transform hologram to hold all the information of the object. In a one-dimensional case, the SBP of the CCD with lateral dimension L_H and a pixel interval of Δx is given by

$$\mathrm{SW}_H = \frac{L_H}{\Delta x} = L_H W_H, \qquad (5)$$

where $W_H = 1/\Delta x$ is the spatial frequency bandwidth of the CCD. If $W_H \geq W$ and $L_H \geq L$ are satisfied, we obtain $\mathrm{SW}_H \geq \mathrm{SW}$. Then all the information for the object can be recorded by the CCD. In fact, a digital holographic system is a low-pass filter because SW_H is always less than the SBP. Then the Nyquist–Shannon sampling theorem, $W_H \geq W$, must be satisfied in the sampling process and the information of the object in the spatial frequency domain should be sampled first. Together with inequality (3) we obtain distance d between the CCD and the object:

$$d \geq \frac{4S_0 \Delta x}{\lambda}. \qquad (6)$$

In lensless Fourier transform holography, the bandwidth of the object will be compressed in the frequency domain and expanded in the spatial domain with increasing d, but the SW of the system will decrease in this process. To record more information, closer recording distance and larger recording area are required in the holographic system when the cutoff frequency of CCD is definite. Increasing the area of the CCD would not result in undersampling the hologram, which could not be avoided in inline and off-axis holography. So it is obvious that the synthetic aperture technique using linear CCD scanning combined with lensless Fourier transform holography should be used to record holograms with a large area.

3. Numerical Reconstruction of Holograms with a Large Area

Because the holograms recorded using the above experimental setup have a larger area than that of a general CCD, the Fresnel approximation would not be satisfied. So the Rayleigh–Sommerfeld integral is required to describe the numerical reconstruction process. Seeing Fig. 3 and supposing the object and the reference source are located in the $x_0 y_0$ plane, and the CCD chip set lies in the $x-y$ plane, the complex amplitude distribution of the object wave in the $x-y$ plane can be written as

$$U(x,y) = \frac{1}{i\lambda}\int\int_{\sum} O(x_0,y_0)\frac{\exp(ikr)}{r}\frac{d}{r}\mathrm{d}x_0\mathrm{d}y_0, \qquad (7)$$

where $O(x_0,y_0)$ is the complex amplitude distribution of the object wave in the x_0–y_0 plane and r is the distance between M_0 and M. Considering that the size and the recording distance of the hologram are much larger than the object size, we have x_0, $y_0 \ll x$, y, and d. So r can be approximated by

$$r \approx [x^2 + y^2 + d^2]^{1/2}\left[1 - \frac{xx_0 + yy_0}{x^2 + y^2 + d^2}\right]. \qquad (8)$$

Defining

$$f_x = \frac{x}{\lambda(x^2 + y^2 + d^2)^{1/2}}, \qquad f_y = \frac{y}{\lambda(x^2 + y^2 + d^2)^{1/2}}, \qquad (9)$$

and taking r into Eq. (7), the $U(x,y)$ can be expressed as

$$U(x,y) = \frac{d\exp[ik(x^2 + y^2 + d^2)^{1/2}]}{i\lambda(x^2 + y^2 + d^2)}O'(f_x,f_y), \qquad (10)$$

where $O'(f_x,f_y)$ is the Fourier transform of $O(x_0,y_0)$. The complex amplitude distribution $R(x,y)$ of the reference source in the $x-y$ plane can also be calculated by

$$R(x,y) = \frac{d\exp[ik(x^2+y^2+d^2)^{1/2}]}{i\lambda(x^2+y^2+d^2)}C, \tag{11}$$

where $C = \exp(j2\pi f_y b)$. And then intensity $I(x,y)$ of the interference fringes in the recording plane is

$$\begin{aligned} I(x,y) &= |U(x,y)+R(x,y)|^2 \\ &= \frac{d^2}{\lambda^2(x^2+y^2+d^2)^2}[C^* O'(f_x,f_y) + CO'^*(f_x,f_y) \\ &\quad + |C|^2 + |O'(f_x,f_y)|^2]. \end{aligned} \tag{12}$$

Equation (12) is the foundation of the reconstruction process. The exact complex amplitude distribution $O(x_0,y_0)$ of the object wave can be obtained by multiplying the intensity $I(x,y)$ with $\lambda^2(x^2+y^2+d^2)^2/d^2$ and then performing the coordinate transform and inverse Fourier transform to the product. A two-dimensional discrete fast Fourier transform (FFT) algorithm can be introduced to obtain a rapid numerical calculation. Therefore the numerical reconstruction of a digital hologram with 5000×5000 pixels recorded by use of linear CCD scanning can be done rapidly on a PC.

From Eqs. (9), the minimum resolvable distance δ of the reconstructed images can be calculated by

$$\delta = \frac{1}{2f} = \lambda\sqrt{\frac{1}{2}+\left(\frac{d}{L_H}\right)^2}. \tag{13}$$

This is consistent with the result obtained by Takaki and Ohzu [5] using the Fresnel–Kirchhoff integral method. The minimum resolvable distance δ versus recording distance d and the CCD size L_H is shown in Fig. 4, where it is obvious that the closer distance and larger area help to achieve the higher SW and hence obtain the smaller minimum resolvable distance and higher resolution.

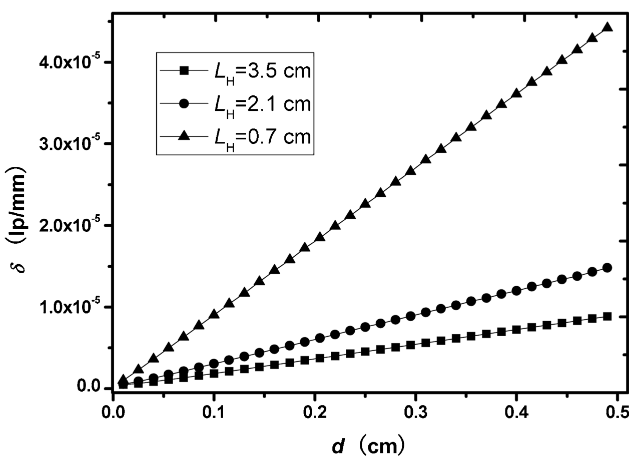

Fig. 4. Minimum resolvable distance δ versus recording distance d and CCD size L_H.

4. Experimental Results

Figure 5 shows the digital lensless Fourier transform hologram with an area of $3.5\,\mathrm{cm}\times3.5\,\mathrm{cm}$ (5000×5000 pixels) recorded based on a synthetic aperture technique and use of linear CCD scanning. The object was a 3# test target with an area of $4\,\mathrm{mm}\times4\,\mathrm{mm}$ and a recording distance d of 14 cm, which is much smaller than the minimum distance required by Fresnel approximation (104 cm). The allowable object size should be $S_0 \le \lambda d/4\Delta x = 0.32\,\mathrm{cm}$ calculated from inequality (6). Figure 6 displays the reconstructed holographic image. Figure 6(a) shows that the zero-order diffraction and the reconstructed images overlap slightly because the size of the 3# test target is slightly larger than S_0. However, the reconstructed images are still clear. According to Eq. (13), the theoretically minimum resolvable distance of the reconstructed images is $2.57\,\mu$m, and the resolution is 194.5 line pairs/mm. Figures 6(b) and 6(c) show the magnified image of grating group 25 in Fig. 6(a). Here the line interval of the smallest element is $5\,\mu$m (i.e., 100 line pairs/mm). The theoretical resolution of the reconstructed image is higher than that of grating group 25, so the gratings along different directions in Fig. 6 can be observed clearly. If the recording distance is shortened to 4.6 cm, the reconstructed image would have a theoretically minimum resolvable distance of less than $1\,\mu$m and a resolution higher than 500 line pairs/mm. In our experiment the resolution of 194.5 line pairs/mm is obtained with a recording distance of 14 cm and a 4 mm field of view. Higher resolution could be obtained if a

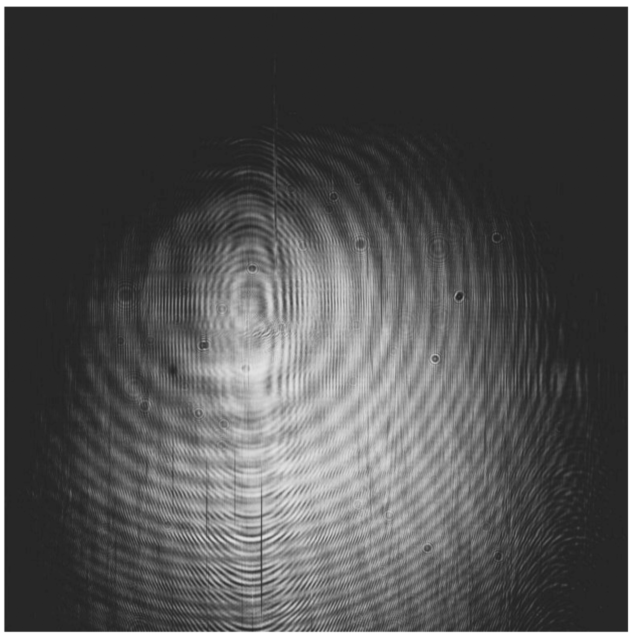

Fig. 5. Digital lensless Fourier transform hologram recorded based on the synthetic aperture technique and use of linear CCD scanning.

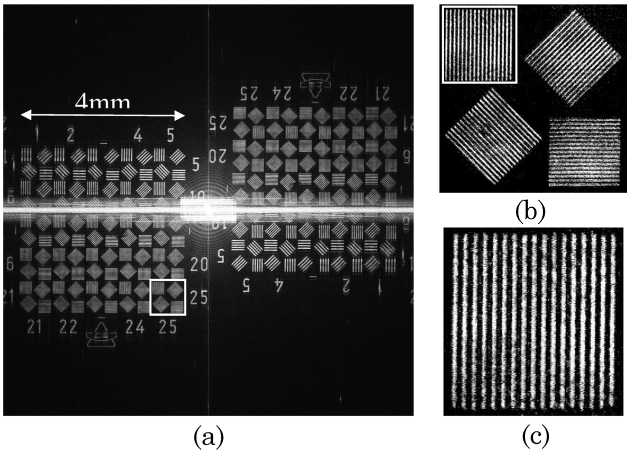

Fig. 6. Reconstructed holographic image: (a) original holographic image; (b) magnification of group 25 in (a); (c) partial magnification of (b).

CCD with more pixels or several CCDs combined were used to record a hologram with a larger area.

In digital lensless Fourier transform holography, the recordable transverse size of the object is directly proportional to the recording distance and the wavelength, and the resolution of the reconstructed image is determined by the recording distance and the hologram size. To record a large object, we must increase the recording distance, which would reduce the resolution of the reconstructed images. Hence the area of the recorded hologram must be increased to obtain a greater SBP and higher resolution when recording a digital hologram under the condition that satisfies spatial frequency domain sampling.

Figure 7 shows the numerical reconstructed results of the holograms for a 2# test target with an area of $2\,\text{mm} \times 2\,\text{mm}$ at different recording distances. Figures 7(a)–7(d) show the holographic images with recording distances d of 17.5, 27.5, 37.5, and 47.5 cm; Figs. 7(e)–7(h) show the amplifications of the corresponding parts in Figs. 7(a)–7(d), respectively. Here the theoretically minimum resolvable distances are 3.20, 4.99, 6.79, and 8.60 μm; the corresponding resolutions are 156.5, 100.2, 73.6, and 58.1 line pairs/mm, respectively. The actual resolutions of the 2# test target are 100, 100, 70.7, and 56.1 line pairs/mm, respectively. It can be seen that the SBP and the resolution of the digital holographic system will reduce when the recording distance is increased, which is consistent with the theoretical results in Fig. 4.

To compare the influence of the hologram sizes on the resolution of the reconstructed holographic images, two small holograms with 3000×3000 pixels and 1000×1000 pixels are cut separately from the center of the hologram (2# test target) recorded by use of linear CCD scanning at distance $d = 17.5$ cm. Figure 8 shows the numerically reconstructed results of two small holograms whose theoretically minimum resolvable distances are 5.29 and 15.83 μm and with resolutions of 94.5 and 31.6 line pairs/mm, respectively, all of which indicates that, by decreasing the hologram area, the SBP and the resolution of the digital holographic system decrease, which is consistent with the theoretical results shown in Fig. 4.

5. Conclusions

Resolution is one of the most important parameters in a digital holographic system. The SBP of the system can be enhanced and the quality of the reconstructed images can be improved by decreasing the

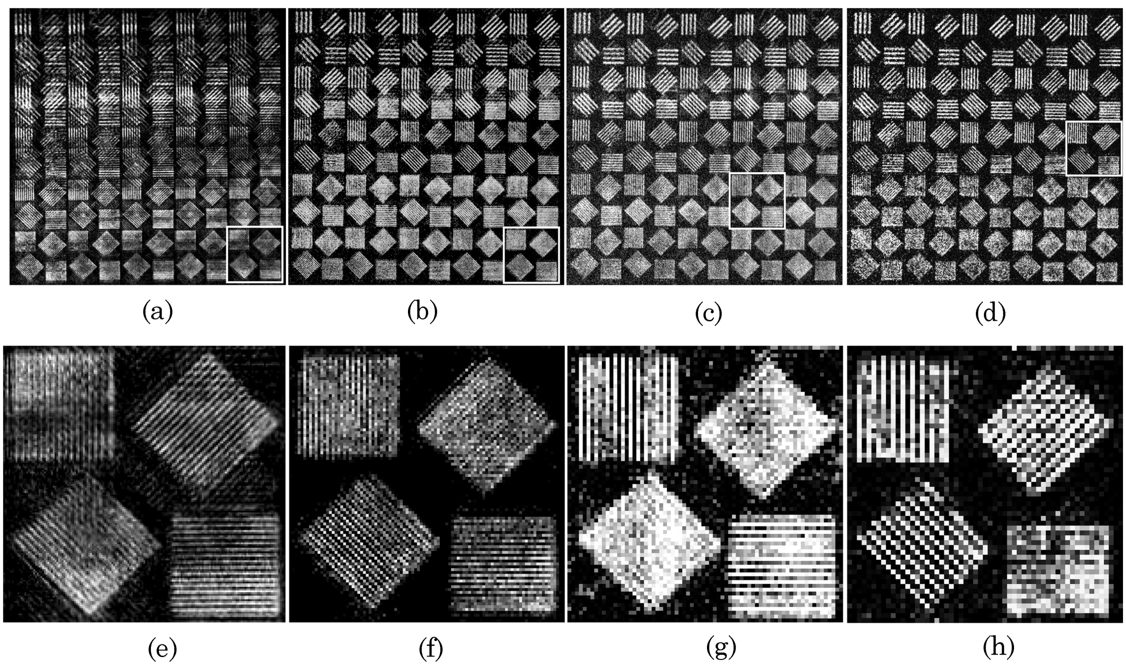

Fig. 7. Reconstruction results for the holograms of a 2# test target recorded at different distances d: (a) 17.5, (b) 27.5, (c) 37.5, (d) 47.5 cm.

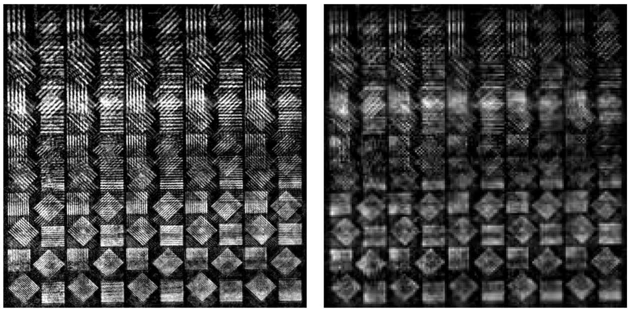

(a) (b)

Fig. 8. Reconstruction results for the holograms of a 2# test target with different numbers of pixels: (a) 3000 x 3000 and (b) 1000 x 1000.

recording distance and increasing the hologram area in digital lensless Fourier transform holography. But a wide field of view needs a long recording distance. To obtain high resolution and a wide field of view, an effective approach is to increase the area and the pixel number of the recorded hologram. In our experiment, we recorded a $3.5\,\mathrm{cm} \times 3.5\,\mathrm{cm}$ lensless Fourier transform hologram by using a synthetic aperture technique based on linear CCD scanning. We have demonstrated the numerical reconstruction result of a 4 mm object at a recording distance of 14 cm by use of a Rayleigh–Sommerfeld integral with a theoretically minimum resolvable distance of $2.57\,\mu\mathrm{m}$. But it should be noted that the synthetic aperture technique and linear CCD scanning can be used only to record a static wave field or a quasi-static wave field because of the limited scanning speed of the mechanical translation stage.

This research is supported by the Science Foundation of Aeronautics of China under grant 2006ZD 53042.

References

1. P. Ferraro, S. De Nicola, G. Coppola, A. Finizio, D. Alfieri, and G. Pierattini, "Controlling image size as a function of distance and wavelength in Fresnel-transform reconstruction of digital holograms," Opt. Lett. **29**, 854–856 (2004).
2. G. Pedrini, W. Osten, and M. E. Gusev, "High-speed digital holographic interferometry for vibration measurement," Appl. Opt. **45**, 3456–3462 (2006).
3. S. A. Alexandrov, T. R. Hillman, T. Gutzler, and D. D. Sampson, "Synthetic aperture fourier holographic optical microscopy," Phys. Rev. Lett. **97**, 168102 (2006).
4. W. Haddad, J. C. S. D. Cullen, J. M. Longworth, A. McPherson, K. Boyer, and C. K. Rhodes, "Fourier-transform holographic microscope," Appl. Opt. **31**, 4973–4978 (1992).
5. Y. Takaki and H. Ohzu, "Fast numerical reconstruction technique for high-resolution hybrid holographic microscopy," Appl. Opt. **38**, 2204–2211 (1999).
6. L. Miccio, D. Alfieri, S. Grilli, P. Ferraro, A. Finizio, L. De Petrocellis, and S. D. Nicola, "Direct full compensation of the aberrations in quantitative phase microscopy of thin objects by a single digital hologram," Appl. Phys. Lett. **90**, 041104 (2007).
7. L. F. Yu, Y. F. An, and L. L. Cai, "Numerical reconstruction of digital holograms with variable viewing angles," Opt. Express **10**, 1250–1257 (2002).
8. E. Cuche, P. Marquet, and C. Depeursinge, "Simultaneous amplitude-contrast and quantitative phase-contrast microscopy by numerical reconstruction of Fresnel off-axis holograms," Appl. Opt. **38**, 6994–7001 (1999).
9. L. F. Yu and Z. P. Chen, "Improved tomographic imaging of wavelength scanning digital holographic microscopy by use of digital spectral shaping," Opt. Express **15**, 878–886 (2007).
10. J. L. Zhao, H. Z. Jiang, and J. L. Di, "Recording and reconstruction of a color holographic image by using digital lensless Fourier transform holography," Opt. Express **16**, 2514–2519 (2008).
11. P. Picart, D. Mounier, and L. M. Desse, "High-resolution digital two-color holographic metrology," Opt. Lett. **33**, 276–278 (2008).
12. L. Hesselink, S. S. Orlov, and M. C. Bashaw, "Holographic data storage systems," Proc. IEEE **92**, 1231–1280 (2004).
13. B. Javidi and D. Kim, "Three-dimensional-object recognition by use of single-exposure on-axis digital holography," Opt. Lett. **30**, 236–238 (2005).
14. A. Stern and B. Lavidi, "Theoretical analysis of three-dimensional imaging and recognition of micro-organisms with a single-exposure on-line holographic microscope," J. Opt. Soc. Am. A **24**, 163–168 (2007).
15. O. Matoba and B. Javidi, "Encrypted optical storage with angular multiplexing," Appl. Opt. **38**, 7288–7293 (1999).
16. J. L. Zhao, H. Q. Lu, X. S. Song, J. F. Li, and Y. H. Ma, "Optical image encryption based on multistage fractional Fourier transforms and pixel scrambling technique," Opt. Commun. **249**, 493–499 (2005).
17. T. C. Poon, K. B. Doh, B. W. Schilling, M. H. Wu, K. K. Shinoda, and Y. Suzuki, "Three-dimensional microscopy by optical scanning holography," Opt. Eng. **34**, 1338–1344 (1995).
18. T. C. Poon, T. Kim, and K. B. Doh, "Optical scanning cryptography for secure wireless transmission," Appl. Opt. **42**, 6496–6503 (2003).
19. T. C. Poon and T. Kim, "Optical image recognition of three-dimensional objects," Appl. Opt. **38**, 370–381 (1999).
20. T. C. Poon, "Recent progress in optical scanning holography," J. Holography Speckle **1**, 6–25 (2004).
21. J. H. Massig, "Digital off-axis holography with a synthetic aperture," Opt. Lett. **27**, 2179–2181 (2002).
22. L. F. Yu and M. K. Kim, "Wavelength-scanning digital interference holography for tomographic three-dimensional imaging by use of the angular spectrum method," Opt. Lett. **30**, 2092–2094 (2005).
23. L. Xu, X. Y. Peng, Z. X. Guo, J. M. Miao, and A. Asundi, "Imaging analysis of digital holography," Opt. Express **13**, 2444–2452 (2005).